




Research Article

Green Synthesis, Characterization and Antioxidant Activity of Chitosan-Coated Iron Oxide Nanoparticles from *Ficus platyphylla*

Abdulrauf Muhammad Shafiu^{1,*}, Abdulhamid Abubakar² , Umar Argungu Aminu² , Aliyu Idris Kankara³ , Musa Fatima¹

¹Department of Biochemistry and Molecular Biology, Federal University, Birnin Kebbi, Nigeria

²Department of Biochemistry, Abdullahi Fodiyo University of Science and Technology, Aliero, Nigeria

³Department of Science Laboratory Technology, Federal Polytechnic, Kaura Namoda, Nigeria

Abstract

Green synthesis using plant extract is an eco-friendly approach for producing metal oxide nanoparticles with improved biological activity. This study investigated the green synthesis of iron oxide nanoparticles (FeONPs) using *Ficus platyphylla* leaf extract and determine how chitosan influences their surface characteristics and antioxidant activity. The FeONPs were synthesized using aqueous *Ficus platyphylla* leaf extract and subsequently coated with a chitosan. The nanoparticles were characterized using UV-visible spectroscopy, Fourier transform infrared spectroscopy (FTIR), X-ray diffraction (XRD) and Scanning electron microscopy (SEM). The antioxidant activity of the aqueous extract was determined using 2, 2-diphenyl-1-picrylhydrazyl (DPPH) free radical scavenging and Ferric reducing antioxidant power (FRAP) assays. The UV-visible spectra confirmed successful nanoparticle formation, while the FTIR showed a strong interaction between chitosan functional groups and iron oxide surface. XRD revealed a highly crystalline cubic spinel structure consistent with magnetite/maghemite and SEM revealed irregular aggregated particles with increased surface roughness after chitosan coating. CS-FeONPs showed significantly higher DPPH scavenging activity ($IC_{50} = 11.63 \pm 0.30 \mu\text{g/mL}$) than uncoated FeONPs ($IC_{50} = 19.53 \pm 0.63 \mu\text{g/mL}$) and the crude extract ($IC_{50} = 23.02 \mu\text{g/mL}$) ($p < 0.05$), approaching the activity of vitamin C. FRAP analysis similarly demonstrated a gradual increased in reducing power from the extract to FeONPs and further to CS-FeONPs. Therefore, combining plant mediated synthesis with chitosan surface functionalization produced a stable iron oxide nanocomposite with improved antioxidant activity. These findings highlighted the role of surface engineering in developing sustainable nanomaterials with promising biomedical applications.

Keywords

Antioxidant Activity, Chitosan, Green Synthesis, Iron Oxide Nanoparticles

1. Introduction

Nanotechnology has become a fundamental driver of innovation in biomedical research by enabling the development of nanoscale materials with improved bioavailability, targeted

*Correspondence: Abdulrauf Muhammad Shafiu (shafiukaura8@gmail.com)

Received: 22 March 2026; Accepted: 7 April 2026; Published: 23 April 2026



Copyright: © The Author(s), 2026. Published by Science Publishing Group. This is an **Open Access** article, distributed under the terms of the Creative Commons Attribution 4.0 License (<http://creativecommons.org/licenses/by/4.0/>), which permits unrestricted use, distribution and reproduction in any medium, provided the original work is properly cited.

biological action and control released [1]. Gradually such systems are being discovered for managing oxidative stress, a fundamental pathological process involved in the progression of many chronic and degenerative diseases. Nanoparticles based platforms offer practical advantage over conventional therapeutic approaches by protecting bioactive compounds from degradation and reducing general toxicity [1]. Iron oxide nanoparticles (FeONPs), specifically magnetite (Fe_3O_4) and hematite ($\alpha\text{-Fe}_2\text{O}_3$), are of particular interest due to their supermagnetic properties, low toxicity and high biocompatibility. These characteristics make them indispensable in biomedical applications such as targeted drug delivery, magnetic resonance imaging (MRI) and hyperthermia therapy [2]. It has also received a considerable attention over other available nanomaterials because of their magnetic properties, favorable biocompatibility and chemical stability [3].

Additionally, iron oxide nanoparticles demonstrate a surface redox behavior that allows interactions with reactive oxygen species, making them relevant for antioxidant related biomedical applications [3]. Since, conventional synthesis method rely on toxic chemicals and energy intensive processes raising biological and environmental safety concerns, green synthesis offers sustainable alternatives. Therefore, green synthesis using plant extract emerged as an environmentally method for nanoparticles production, because plant mediated method proceed under minor conditions and leave surface bound phytochemicals that can improved biological activity, with antioxidant potentials [4].

The antioxidant activity of such green synthesized nanoparticles depends strongly on the phytochemical profile of the plant source used as reducing and capping agent. The genus *Ficus* (Family moraceae) is globally recognized for its rich pharmacological profile and abundance of bioactive compounds. Previous research on *Ficus carica* has successfully demonstrated that fruit and leaf extracts, which are rich in phenols, flavonoids and tannins can efficiently synthesized iron oxide nanoparticles with significant antioxidant and antimicrobial activities [2, 5] *Ficus platyphylla*, locally known as “Gamjiu” in West Africa is a prominent medicinal plant folklore for treating epilepsy, diabetes, wounds and inflammation. Scientific screenings have confirmed that its leaves and bark are exceptionally rich in tannins, saponins and flavonoids [6, 7]. It is also reported to contain phenolic and flavonoid constituents with *in vitro* free radical scavenging activity, recommending its power to act both as reducing/stabilizing agent and as source of surface bound antioxidant for nanoparticles synthesis [8]. Surface engineering provide an additional way to change nanoparticles redox behavior. Chitosan biodegradable polysaccharides with amino acids and hydroxyl group capable of donating electrons, chelating pro-oxidant and scavenging reactive oxygen species, properties makes chitosan a logical choice for improving nanoparticles antioxidant performance [9]. Therefore, this study tested the hypothesis that chitosan functionalization enhances the antioxidant activity iron oxide nanoparticles

synthesized using *Ficus platyphylla* leaf extract. The nanoparticles were synthesized coated with chitosan and physicochemically characterized, followed by evaluation of their antioxidant potential using standardized *in vitro* free radical scavenging and reducing power assays. These assays were used as first line screening tools to establish antioxidant capacity prior to future cellular or *in vivo* validation.

2. Materials and Methods

2.1. Chemicals and Reagents

Ferrous sulfate heptahydrate ($\text{FeSO}_4 \cdot 7\text{H}_2\text{O}$), $\text{FeCl}_3 \cdot 6\text{H}_2\text{O}$, chitosan (low molecular weight; degree of deacetylation 70–90%), 2, 2-diphenyl-1-picrylhydrazyl (DPPH), sodium hydroxide (NaOH), acetic acid, and Mueller–Hinton agar were obtained from Hali Shuaibu Laboratories Store, Sokoto, Nigeria. All other chemicals and reagents used in this study were of analytical grade and were used without further purification. Double-distilled water was used throughout the experiments.

2.2. Green Synthesis of Iron Oxide Nanoparticles (FeO NPs)

The synthesis of Fe_3O_4 -NPs was carried out by a simple and cost-effective co-precipitation technique [10]. A 200mL mixture of precursor salt solution of 1 mM $\text{FeCl}_3 \cdot 6\text{H}_2\text{O}$ and 1 mM $\text{Fe}_2\text{SO}_4 \cdot 7\text{H}_2\text{O}$ (1: 1 v/v) was taken in a 500-mL conical flask and heated at 80.0°C on the electric hot plate. After that, 100 mL of prepared leaf extract of *Ficus platyphylla* was added dropwise by conical flask with continuous stirring at 100 rpm. The addition of *Ficus platyphylla* leaves to extract the light brown color solution started to change into blackish suspension, indicating the formation of Fe_3O_4 -NPs. After 2.0 h, the resulting suspension was cooled at room temperature and filtered with Whatman filter paper. The obtained particles were washed by DIW followed by ethanol to remove impurities and dried in an electric oven at 105°C to get a result of a dark black colored powder. The resulting powder was calcinated in a muffle furnace at 600°C for 4 h to oxidize the organic compounds, and pure Fe_3O_4 -NPs were obtained. The resulting Fe_3O_4 -NPs were characterized by various analytical techniques to study their morphological and structural characteristics.

2.3. Preparation of Chitosan-Coated Iron Oxide Nanocomposite (CS–FeON)

Chitosan-coated iron oxide nanoparticles (CS–FeO) were prepared by surface functionalization of the synthesized FeO NPs. Approximately 200 mg of FeO NPs were dispersed in 20 mL of chitosan solution (prepared by dissolving 20 mg of chitosan in 20 mL of 1% acetic acid). The suspension was stirred

continuously at room temperature for 2 h to facilitate adsorption and interaction between chitosan functional groups and the nanoparticle surface. The resulting nanocomposite was collected using a magnetic separator, washed thoroughly with double-distilled water to remove excess chitosan, and dried at 60°C for 24 h. The dried CS–FeO nanocomposite was stored in a desiccator until further use [11].

2.4. Characterization of Synthesized Nanoparticles

The synthesized FeO NPs and CS–FeO nanocomposites were characterized to evaluate their optical properties, structural features, and surface chemistry. Characterization techniques included UV–visible spectroscopy, Fourier-transform infrared (FTIR) spectroscopy, X-ray diffraction (XRD), and scanning electron microscopy (SEM), as described in the Results section. These analyses were employed to confirm nanoparticle formation, crystallinity, functional group interactions, and morphological features [12].

$$\text{DPPH free radical scavenging (\%)} = \frac{\text{Absorbance}_{\text{control}} - \text{Absorbance}_{\text{Sample}}}{\text{Absorbance}_{\text{control}}} \times 100$$

where

A_{control} = absorbance of the DPPH control

A_{sample} = absorbance of the test sample

The IC_{50} value, defined as the concentration required to scavenge 50% of DPPH radicals, was determined from a plot of percentage inhibition versus sample concentration.

2.6. Ferric Reducing Antioxidant Power (FRAP) Assay

The ferric reducing antioxidant power of *Ficus platyphylla* extract and its nanoparticle formulations were determined using the FRAP assay, following the method described by Benzie and Strain [14]. The FRAP working reagent was freshly prepared by mixing acetate buffer (300 mM, pH 3.6), TPTZ solution (10 mM in 40 mM HCl), and ferric chloride solution (20 mM) in a ratio of 10: 1: 1 (v/v/v) and pre-warmed to 37°C. For the assay, 100 μL of each test sample was added to 3.0 mL of the FRAP reagent in clean test tubes. The mixtures were vortexed gently and incubated at 37°C for 30 min to allow reduction of Fe^{3+} to Fe^{2+} . Absorbance was then measured at 593 nm using a UV–visible spectrophotometer. FRAP values were calculated from a calibration curve constructed using ferrous sulfate and expressed as $\mu\text{mol Fe}^{2+}$ equivalents per gram of sample.

2.7. Statistical Analysis

All experiments were performed in triplicate, and results are expressed as mean \pm standard deviation (SD). Statistical significance between groups was evaluated using one-way analysis of variance (ANOVA), followed by Tukey's post hoc

2.5. 2, 2-Diphenyl-1-Picrylhydrazyl (DPPH) Free Radical Scavenging Assay

The antioxidant activity of *Ficus platyphylla* leaf extract and its nanoparticle formulations were evaluated using the DPPH free radical scavenging assay, adapted from the method of [13]. This assay measures the ability of test samples to donate hydrogen atoms or electrons to neutralize the stable DPPH radical. Briefly, 1.0 mL of freshly prepared DPPH solution was mixed with 1.0 mL of each test sample at different concentrations in clean test tubes. The mixtures were vortexed gently and incubated in the dark at room temperature for 30 min. Following incubation, absorbance was measured at 517 nm using a UV–visible spectrophotometer. A mixture of methanol and DPPH solution served as the control, while methanol alone was used as the blank. The percentage DPPH radical scavenging activity was calculated using the equation:

Calculation

The percentage DPPH radical scavenging activity was calculated using the equation:

test. Differences were considered statistically significant at $p < 0.05$.

3. Results

3.1. Visual and Physicochemical Characterization

The formation of iron oxide nanoparticles (FeONPs) was initially confirmed by a distinct color change of the reaction mixture from yellow to black, demonstrating phytochemical-mediated reduction of iron ions and nanoparticle nucleation. Following chitosan functionalization, the nanoparticles displayed a brownish coloration, consistent with the formation of a polymer-coated nanocomposite as shown in Figure 1 below:



Figure 1. Synthesized nanoparticles: (a) FeONPs and (b) chitosan-coated iron oxide nanoparticles (CS–FeONP).

3.2. UV-Visible Spectroscopy

UV-visible spectral analysis confirmed the formation of FeONPs through extracellular reduction of Fe^{2+} ions (Figure 2). The FeONPs displayed a broad absorption band in the near-ultraviolet region (346–369 nm), it is attributed to ligand-to-metal charge transfer transitions, along with weak absorption features in the visible region (664–672 nm), and associated with surface defect states. After chitosan coating, a slight redshift and broadening of the near-UV band were observed, accompanied by attenuation of visible absorption.

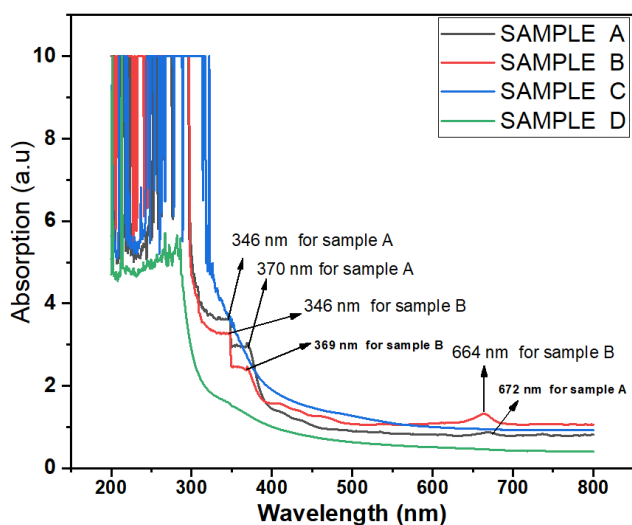


Figure 2. UV-Vis absorption spectra of (a) CS-FeONP (black), (b) FeONPs (red), (c) *Ficus platyphylla* extract (blue), and (d) pure chitosan (green).

3.3. Fourier Transform Infrared (FTIR) Spectroscopy

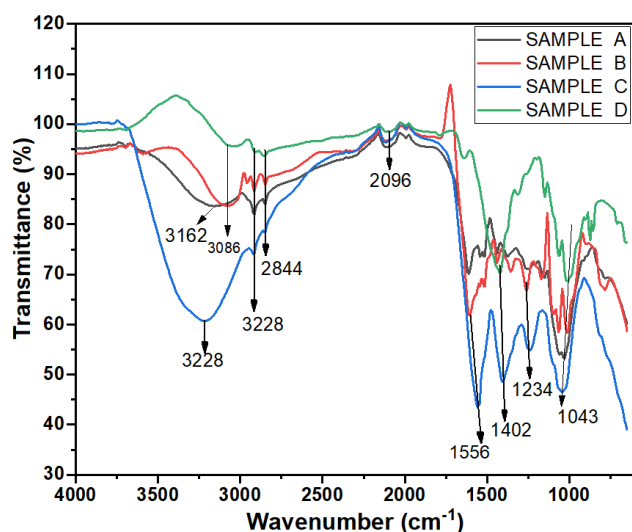


Figure 3. FTIR spectra of (a) CS-FeONP, (b) FeONPs, (c) plant extract, and (d) pure chitosan.

FTIR spectra (Figure 3) revealed functional groups interactions and confirmed successful chitosan coating. Pure chitosan exhibited broad O-H/N-H stretching vibrations around 3228 cm^{-1} and characteristic polysaccharide bands in the $1200\text{--}1000\text{ cm}^{-1}$ region. The FeONPs showed weak organic bands attributable to surface-bound phytochemicals from *Ficus platyphylla*. In contrast, CS-FeONP spectra displayed the band broadening and slight shifts in chitosan-associated peaks, indicating hydrogen bonding and coordination interactions between chitosan functional groups and $\text{Fe}^{2+}/\text{Fe}^{3+}$ ions. Prominent Fe-O lattice vibrations in the $500\text{--}600\text{ cm}^{-1}$ region confirmed the presence of an iron oxide core.

3.4. X-Ray Diffraction (XRD) Analysis

XRD patterns (Figure 4) showed that the synthesized FeONPs possess a cubic spinel structure characteristic of magnetite or maghemite ($\text{Fe}_3\text{O}_4/\gamma\text{-Fe}_2\text{O}_3$). Diffraction peaks observed at 2θ values of 30.1° , 35.5° , 43.1° , 53.4° , 57.0° , and 62.6° corresponded to the (220), (311), (400), (422), (511), and (440) planes, respectively. The CS-FeONP samples revealed broadened diffraction peaks with an elevated amorphous background in the $18\text{--}25^\circ$ 2θ range, reflecting polymer encapsulations of the crystalline core.

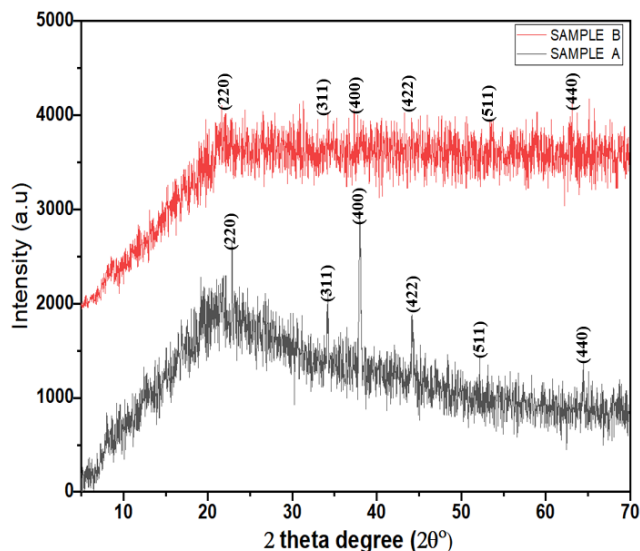


Figure 4. XRD patterns of (a) CS-FeONP and (b) FeONPs.

3.5. Scanning Electron Microscopy (SEM)

SEM micrographs showed irregular and aggregated particle morphologies for both FeONPs and CS-FeONP. The aggregation is attributed to magnetic dipole-dipole interactions inherent to iron oxide nanoparticles. Chitosan-coated nanoparticles exhibited increased surface roughness compared to uncoated FeONPs, consistent with polymer deposition on the nanoparticle surface. This enhanced surface texture may contrib-

ute to improved surface reactivity and antioxidant performance.

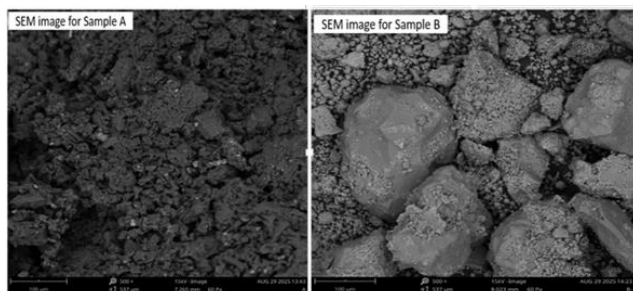


Figure 5. SEM micrographs of (a) CS-FeONP and (b) FeONPs showing irregular particles, block-like agglomerates and surface roughness.

3.6. DPPH Free Radical Scavenging Activity

The DPPH free radical scavenging assay showed a statistically significant increase in antioxidant activity following nanoparticle formulation ($p < 0.05$). The CS-FeONP exhibited the lowest IC_{50} value ($11.63 \pm 0.30 \mu\text{g/mL}$), followed by FeONPs ($19.53 \mu\text{g/mL}$), while the crude *Ficus platyphylla* extract showed the highest IC_{50} value ($30.91 \pm 1.32 \mu\text{g/mL}$). But, Vitamin C displayed the strongest scavenging activity with an IC_{50} value of ($2.23 \pm 0.11 \mu\text{g/mL}$). The order of DPPH scavenging activity was vitamin C > CS-FeONP > FeONP > crude extract as shown in Table 1.

Table 1. IC_{50} values of DPPH radical scavenging activity of *Ficus platyphylla* and its Nanoparticle Formulations.

Sample	DPPH ($\mu\text{g/mL}$)
FP (Extract)	$30.91 \pm 1.32a$
FeONP	$19.53 \pm 0.63b$
CS-FeONP	$11.63 \pm 0.30c$
Vit. C	$2.23 \pm 0.11d$

Values were expressed as mean \pm standard deviation ($n = 3$). Means with different superscript letters are significantly different at $p < 0.05$ according to one-way ANOVA followed by Tukey's post-hoc test.

3.7. Ferric Reducing Antioxidant Power (FRAP) of *Ficus platyphylla* and Its Nanoparticle Formulations

The FRAP assay revealed significant differences in reducing power among the samples ($p < 0.05$). The crude *Ficus platyphylla* extract showed the lowest FRAP value ($99.54 \pm 0.38 \mu\text{mol Fe}^{2+}/\text{g}$), while FeONPs exhibited a higher reducing

capacity ($105.88 \pm 2.84 \mu\text{mol Fe}^{2+}/\text{g}$). CS-FeONP recorded the highest FRAP value among the plant-derived samples ($127.96 \pm 1.26 \mu\text{mol Fe}^{2+}/\text{g}$), whereas vitamin C showed the highest overall reducing power ($134.79 \pm 1.63 \mu\text{mol Fe}^{2+}/\text{g}$) as shown in Table 2 below.

Table 2. Ferric reducing antioxidant power of *Ficus platyphylla* and its nanoparticle formulations.

Sample	FRAP ($\mu\text{mol Fe}^{2+}/\text{g}$)
FP (Extract)	$99.54 \pm 0.38a$
FeONP	$105.88 \pm 2.84b$
CS-FeONP	$127.96 \pm 1.26c$
Vitamin C	$134.79 \pm 1.63d$

Values were expressed as mean \pm standard deviation ($n = 3$). Means with different superscript letters are significantly different at $p < 0.05$ according to one-way ANOVA followed by Tukey's post-hoc test.

4. Discussion

The green synthesis of iron oxide nanoparticles (FeONPs) using *Ficus platyphylla* leaf extract was demonstrated by characteristic color change from yellow to black, indicating phytochemical-mediated reduction and nucleation at the nanoscale. Plant derived-polyphenols and related secondary metabolites are known to function as both reducing and stabilizing agents, enabling environmentally benign nanoparticles formation while modulating surface chemistry and biological activity [15, 16]. After chitosan functionalization a brown coloration was produced, consistent with polymer shell formation around the iron oxide core and successful surface modification. Comparable observations have been reported in a studies where chitosan was used encapsulate or functionalize magnetic nanoparticles reinforcing nanothe interpretation that the biopolymer successfully coated the particle surface [17]. UV-visible spectroscopy confirmed nanoparticle formation through absorption features associated with nanoscale iron oxide and $\text{Fe}^{2+}/\text{Fe}^{3+}$ charge transfer transitions. Redshift and band broadening after chitosan coating indicated surface passivation and altered local electronic environments, supporting effecting polymer nanoparticle interactions [18]. FTIR spectra further validated nanoparticle formation by revealing Fe---O vibration alongside broadened O---H and N---H bands, confirming strong interactions between chitosan functional group and iron oxide surface [19, 20]. Similar interactions between polymer functional groups and iron oxide surfaces have been reported across several studies on chitosan stabilized nanoparticles, emphasizing the effectiveness of the chitosan as a coated material that enhances colloidal material that introduce reactive functional groups for drug delivery or catalytic applications [20, 21]. X-ray diffraction patterns confirmed a cubic spinel structure (magnetite or maghemite) with

high crystallinity and no detectable impurities. Reduced diffraction intensity and increased amorphous background after chitosan coating are consistent with polymer encapsulation of the crystalline core. SEM analysis revealed irregular, agglomerated morphologies attributable to magnetic dipole–dipole interactions. Increased surface roughness following chitosan coating suggests enhanced surface functionality and reactivity [21, 22]. The irregular and blocked like morphologies align with previous findings in green synthesized iron oxide nanoparticles, where rapid nucleation induced by plant phytochemicals often yields polydispersed particles with rough surface [23, 24]. Iron oxide nanoparticles can show both antioxidant and pro-oxidant depending on surface chemistry, the observed phytochemical capping and chitosan functionalization likely shift redox behavior toward antioxidant activity by stabilizing the surface and facilitating controlled electron transfer. Antioxidant evaluation demonstrated a progressive enhancement in redox reactivity from crude plant extract to FeONPs and further to chitosan coated FeONPs. This trend reflect synergistic contributions from nanoscale effects, surface bound phytochemicals retained during green synthesis, and intrinsic electron donating and metal chelating properties of chitosan [24, 25]. The in vitro antioxidant assays employed served as first-line screening tools, providing mechanistic insight into free radical scavenging and reducing power capacity prior to future biological validations.

5. Conclusion

The green synthesis using *Ficus platyphylla* leaf extract combined with chitosan coating, resulted in iron oxide nanoparticles that are both stable and biocompatible. The natural phytochemicals and chitosan layer worked together to improved surface characteristic, strengthen structural stability and enhance antioxidant activity. The gradual development in redox performance from the crude plant extract to the coated nanoparticles shows how nanoscale properties and surface modification can act synergistically underscoring the value of surface engineering in designing sustainable iron oxide nanomaterials with promising biomedical applications.

Abbreviations

FeONP	Iron Oxide Nanoparticle
CS-FeONP	Chitosan Iron Oxide Nanoparticle
XRD	X-Ray Diffraction
SEM	Scanning Electron Microscopy
FTIR	Fourier Transform Infrared
DPPH	2, 2-diphenyl-1-picrylhydrazyl
FRAP	Ferric Reducing Antioxidant Power
FP	<i>Ficus platyphylla</i>
UV	UltraViolet
ANOVA	Analysis of Variance
SD	Standard Deviation

Author Contributions

Abdulrauf Muhammad Shafiu: Conceptualization, Methodology, Writing – original draft

Abdulhamid Abubakar: Supervision, Validation

Umar Argungu Aminu: Supervision, Validation

Aliyu Idris Kankara: Data curation, Formal Analysis

Musa Fatima: Formal Analysis

Conflicts of Interest

Authors have declared that no competing interests exist.

References

- [1] Jiang, K., Zhang L. and Bao G. (2021). Magnetic iron oxide nanoparticles for biomedical applications: synthesis, coating and applications. *Frontiers / relevant journal* (review).
- [2] Ustun E., Onbas S. C., Celik S. K., Ayvaz M. C. and Sahin N. (2021). Green synthesis of iron oxide nanoparticles by using *Ficus carica* leaf extract and its antioxidant activity. *Biointerface Research in Applied Chemistry* 12(2), 2108-2116 <https://doi.org/10.33263/BRIAC122.21082116>
- [3] Montiel Schneider, M. G., Julia Martin M., Otarola J., Vakarelska E., Simeonov V., Lassalle V. and Nedyalkova M. (2022). Biomedical applications of iron oxide nanoparticles: a review. *Pharmaceutics*, 14(1), 204. <https://doi.org/10.3390/pharmaceutics14010204>
- [4] Zúñiga-Miranda, J., Guerra J., Muella A., Mayorga-Ramus A., Carrera Pacheco S. E., Barba-Ostria C., Heredia-Moya J. and Guaman L. P. (2023). Iron oxide nanoparticles: green synthesis methods and biological activity review. *Nanomaterials*.
- [5] Demirezen, D. A., Yildiz, Y. S., Yilmaz, S., and Yilmaz, D. D. (2019). Green synthesis and characterization of iron oxide nanoparticles using *Ficus carica* (common fig) dried fruit extract. *Journal of Bioscience and Bioengineering*, 127(2), 241-245 <https://doi.org/10.1016/j.jbiosc.2018.07.024>
- [6] Shemishere, U. B., Turaki A. A., Yusuf A. B., Anyebe D. A. and Erhovwosere O. (2023). Phytochemical constituents and free radical scavenging activities of methanol extract and fractions of *Ficus platyphylla* leaves. *FUDMA Journal of Sciences*, 7(5), 369-376 <https://doi.org/10.33003/fjs-2023-0705-1973>
- [7] Chindo, B. A., Joseph A. A. and Karniyu S. G (2012). Toxicity studies of the standardized extract of *Ficus platyphylla* stem bark in rodents. *Journal of Ethnopharmacology*, 144(1), 155-159 <https://doi.org/10.5567/PHARMACOLOGIA.2012.499.505>
- [8] Hassan, M., Bala S. Z., Bashir M., Waziri P, M., Adam R. M., Umar M. A. and Kini P. (2022). LC-MS and GC-MS profiling of different fractions of *Ficus platyphylla*: phytochemical composition and antioxidant properties. *Journal of Analytical Method in Chemistry* 14; 2022: 6349332. <https://doi.org/10.1155/2022/6349332>

- [9] Ivanova, D. G. (2020). Antioxidant properties and redox-modulating activity of chitosan and its derivatives: potential applications. *BioResearch Open Access*.
<https://doi.org/10.1089/biores.2019.0028>
- [10] Kaushik, A., Solanki P. R., Ansari A. A., Sumana G., Ahmad S. and Malhotra B. D. (2009).: Iron oxide-chitosan nanobiocomposite for urea sensor. *Sens. Actuators B Chem.* 138(2), 572-580 <https://doi.org/10.1016/j.snb.2009.02.005>
- [11] Bharathi D., Ranjithkumar R., Vasantharaj S., Chandarshekar B. and Bhuvaneshwari V. (2019). Synthesis and characterization of chitosan/iron oxide nanocomposite for biomedical applications. *International Journal of Biological Macromolecules*, 132, 880-887,
<https://doi.org/10.1016/j.ijbiomac.2019.03.233>
- [12] Brahman, K. D., Kazi T. G., Afridi H. I., Baig J. A., Abro M. I., Arain S. S., Ali J. and Khan S. (2016). Simultaneously removal of inorganic arsenic species from stored rainwater in arsenic endemic area by leaves of *Tecomella undulata*: a multivariate study. *Environmental Science Pollution Research* 23(15), 15149-15163
<https://doi.org/10.1007/s11356-016-6519-2>
- [13] Brand-Williams, W., Cuvelier, M. E. and Berset, C. L. W. T. (1995) Use of a Free Radical Method to Evaluate Antioxidant Activity. *LWT-Food Science and Technology*, 28, 25-30.
[http://dx.doi.org/10.1016/S0023-6438\(95\)80008-5](http://dx.doi.org/10.1016/S0023-6438(95)80008-5)
- [14] Benzie, i. f. f., and Strain, j. j. (1996). The ferric reducing ability of plasma (frap) as a measure of "antioxidant power": the frap assay. *analytical biochemistry*, 239(1), 70-76.
<https://doi.org/10.1006/abio.1996.0292>
- [15] Cornell, R. M., and Schwertmann, U. (2023). *The Iron Oxides* (3rd ed.). Wiley-VCH.
- [16] Bhutto A. A., Baig J. A., Uddin S., Kazi T., Sierra-Alvarez R. (2023) Biosynthesis and Analytical Characterization of Iron Oxide Nanocomposite for In-Depth Adsorption Strategy for Removal of Toxic Metals of Toxic Metals from Drinking Water. *Arabian Journal for Science and Engineering* 296, 127193.
<https://doi.org/10.1007/s13369-022-07477-y>
- [17] Nehra, P., Chauhan, R. P., Garg, N., and Verma, K. (2018). Antibacterial and antifungal activity of chitosan-coated iron oxide nanoparticles. *British Journal of Biomedical Science*, 75, 13-18. <https://doi.org/10.1080/09674845.2017.1347362>
- [18] Pham, X. N., Nguyen N. H., Phan T. B. P., Ha T. B. H., Nguyen X. P. and Phan B. T. (2021). Polymer-functionalized iron oxide nanoparticles. *Colloids and Surfaces B: Biointerfaces*, 197, 111396. <https://doi.org/10.1016/j.colsurfb.2020.111396>
- [19] Asab, G., Zereffa, E. A., and Seghne, T. A. (2020). Plant-mediated synthesis of metal and metal oxide nanoparticles. *Green Chemistry Letters and Reviews*, 13, 236-256.
<https://doi.org/10.1080/17518253.2020.1814893>
- [20] Perez, A. G., Martinez E. G., Aguila C. D., Martinez D. G., Ruiz G. G., Artalejo A. G. and Madera H. Y. (2020). Chitosan-coated magnetic nanoparticles for biomolecule separation. *Colloids and Surfaces A*, 591, 124500.
- [21] Dhavale, R. P., Nisar, S., and Patil, S. P. (2021). Chitosan-functionalized magnetic nanoparticles. *International Journal of Biological Macromolecules*, 183, 189-204.
<https://doi.org/10.1016/j.ijbiomac.2021.05.029>
- [22] Sarasithiyankam, N., Uematsu Y., Ogata F., Saenjum C., Nakamura T and Kawasaki N. (2020). Chitosan-based magnetic nanocomposites. *Carbohydrate Polymers*, 241, 116345.
- [23] Muhammed, A., and Abdullahi, A. (2018). Scanning electron microscopy: A review. In *Proceedings of HERVEX 2018* (pp. 7-9).
- [24] Mirza, A. U., Kareem A., Nami S. A. A., Khan M. S., Rehman S., Bhat S. A., Mohammad A., and Nishat N. (2018). Biogenic synthesis of iron oxide nanoparticles. *Journal of Photochemistry and Photobiology*, 185, 262-274.
<https://doi.org/10.1016/j.jphotobiol.2018.06.009>
- [25] Ahmed, S., Ahmad, M., Swami, B. L., and Ikram, S. (2021). Green synthesis of metal nanoparticles using plant extracts: A review. *Journal of Advanced Research*, 28, 1-17.
<https://doi.org/10.1016/j.jare.2015.02.007>